

Formal Verification of Probabilistic Multi-Agent Systems for Ballistic Rocket Flight Using Probabilistic Alternating-Time Temporal Logic

Damian Kurpiewski^{1,2}, Jędrzej Michalczyk³, Wojciech Jamroga^{1,2},
Jerzy Julian Michalski³, and Teofil Sidoruk¹

¹*Institute of Computer Science, Polish Academy of Sciences*

²*Nicolaus Copernicus University in Toruń, Poland*

³*SpaceForest Sp. z o.o., Gdynia, Poland*

Abstract

This technical report presents a comprehensive formal verification approach for probabilistic agent systems modeling ballistic rocket flight trajectories using Probabilistic Alternating-Time Temporal Logic (PATL). We describe an innovative verification framework specifically designed for analyzing critical safety properties of ballistic rockets engineered to achieve microgravity conditions for scientific experimentation. Our model integrates authentic flight telemetry data encompassing velocity vectors, pitch angles, attitude parameters, and GPS coordinates to construct probabilistic state transition systems that rigorously account for environmental stochasticity, particularly meteorological variability. We formalize mission-critical safety properties through PATL specifications to systematically identify trajectory deviation states where the rocket risks landing in prohibited or hazardous zones. The verification framework facilitates real-time safety monitoring and enables automated intervention mechanisms, including emergency engine disengagement protocols, when predefined safety thresholds are exceeded. Experimental validation demonstrates the practical effectiveness and reliability of our approach in ensuring mission safety while maintaining scientific mission objectives.

1 Introduction

Many important properties of agent systems refer to *strategic abilities* of agents and their groups. *Alternating-time temporal logic* **ATL**^{*} [3, 27] and *Strategy Logic*

SL [26] provide powerful tools to reason about such aspects of MAS. For example, the **ATL**^{*} formula $\langle\langle taxi \rangle\rangle G \neg \text{fatality}$ expresses that the autonomous cab can drive in such a way that no one gets ever killed. Similarly, $\langle\langle taxi, passg \rangle\rangle F \text{ destination}$ says that the cab and the passenger have a joint strategy to arrive at the destination, no matter what the other agents do. Specifications in agent logics can be used as input to algorithms and tools for *model checking*, that have been in constant development for over 20 years [2, 10, 11, 18, 24, 25].

Model checking of strategic abilities is hard, both theoretically and in practice. First, it suffers from the well-known state/transition-space explosion. Moreover, the space of possible strategies is at least exponential *on top of the state-space explosion*, and incremental synthesis of strategies is not possible in general – especially in the realistic case of agents with partial observability. Even for the more restricted (and computation-friendly) logic **ATL**, model checking of its imperfect information variants is Δ_2^P - to **PSPACE**-complete for agents playing memory-less strategies [8, 27] and **EXPTIME**-complete to undecidable for agents with perfect recall [14, 16]. The theoretical results concur with outcomes of empirical studies on benchmarks [10, 21, 25], as well as recent attempts at verification of real-life multi-agent scenarios [20, 23].

This technical report presents a comprehensive case study demonstrating the application of state-of-the-art strategy synthesis techniques to the Perun Rocket system developed by SpaceForest. This work represents a significant methodological advancement as we bridge the gap between cutting-edge theoretical research in formal verification and real-world aerospace engineering challenges. The case study exemplifies the practical deployment of highly experimental and innovative formal methods (specifically, probabilistic model checking and strategic reasoning in agent systems) to a genuine aerospace scenario with critical safety requirements.

The verification of rocket flight systems poses unique challenges that distinguish it from traditional software verification tasks. Unlike conventional computational systems, ballistic rockets operate in highly dynamic, uncertain environments where atmospheric conditions, mechanical tolerances, and sensor inaccuracies introduce substantial stochasticity. Furthermore, the multi-agent perspective becomes crucial when considering the rocket’s control systems, environmental factors, and ground-based monitoring as interacting entities whose collective behavior determines mission success or failure.

Our approach leverages PATL to express and verify complex strategic properties about what the rocket’s control systems can achieve under various probabilistic scenarios. This enables us to reason formally about questions such as: “Can the flight control system guarantee with probability at least p that the rocket will remain within safe trajectory bounds?”.

The integration of formal methods with aerospace engineering represents not

only a technical challenge but also an opportunity to establish new standards for safety verification in the emerging commercial space industry.

2 What Agents Can Achieve

In this section, we introduce the formalism of Asynchronous Multi-agent Systems (AMAS) [19], as well as the syntax and semantics of Alternating-time Temporal Logic **ATL**^{*} [3, 27], which allows for specifying relevant properties of SAI models, in particular the *strategic ability* of agents to enforce a goal.

2.1 Asynchronous MAS

AMAS can be thought of as networks of automata, where each component corresponds to a single agent.

Definition 1 (AMAS [19]) *An asynchronous multi-agent system (AMAS) consists of n agents $\mathcal{A} = \{1, \dots, n\}$, each associated with a 7-tuple $A_i = (L_i, \iota_i, Evt_i, R_i, T_i, PV_i, V_i)$, where:*

- $L_i = \{l_i^1, \dots, l_i^{n_i}\} \neq \emptyset$ is a finite set of local states;
- $\iota_i \in L_i$ is an initial local state;
- $Evt_i = \{e_i^1, \dots, e_i^{m_i}\} \neq \emptyset$ a finite set of events;
- $R_i : L_i \rightarrow 2^{Evt_i} \setminus \{\emptyset\}$ is a repertoire of choices, assigning available subsets of events to local states;
- $T_i : L_i \times Evt_i \rightharpoonup L_i$ is a (partial) local transition function such that $T_i(l_i, e)$ is defined iff $e \in R_i(l_i)$. That is, $T_i(l, e)$ indicates the result of executing event e in state l from the perspective of agent i ;
- PV_i is a set of the agent's local propositions, with PV_j, PV_k (for $j \neq k \in \mathcal{A}$) assumed to be disjoint;
- $V_i : L_i \rightarrow \mathcal{P}(PV_i)$ is a valuation function.

Furthermore, we denote:

- by $Evt = \bigcup_{i \in \mathcal{A}} Evt_i$, the set of all events;
- by $L = \bigcup_{i \in \mathcal{A}} L_i$, the set of all local states;

- by $\text{Agent}(e) = \{i \in \mathcal{A} \mid e \in \text{Evt}_i\}$, the set of all agents which have event e in their repertoires;
- by $PV = \bigcup_{i \in \mathcal{A}} PV_i$ the set of all local propositions.

The *model* of an AMAS provides its execution semantics with asynchronous interleaving of private events and synchronisation on shared ones.

Definition 2 (Model) *The model of an AMAS is a 5-tuple $M = (\mathcal{A}, S, \iota, T, V)$, where:*

- \mathcal{A} is the set of agents;
- $S \subseteq L_1 \times \dots \times L_n$ is the set of global states, including all states reachable from ι by T (see below);
- $\iota = (\iota_1, \dots, \iota_n) \in S$ is the initial global state;
- $T : S \times \text{Evt} \rightharpoonup S$ is the global transition function, defined by $T(q_1, e) = q_2$ iff $T_i(q_1^i, e) = q_2^i$ for all $i \in \text{Agent}(e)$ and $q_1^i = q_2^i$ for all $i \in \mathcal{A} \setminus \text{Agent}(e)$ (where $q_j^i \in L_i$ is agent i 's local component of q_j);
- $V : S \rightarrow 2^{PV}$ is the global valuation function, defined as $V(l_1, \dots, l_n) = \bigcup_{i \in \mathcal{A}} V_i(l_i)$.

2.2 Strategic Ability

Linear and branching-time temporal logics, such as **LTL** and **CTL*** [15], have long been used in formal verification. They enable to express properties about *how* the state of the system will (or should) evolve over time. However, in systems that involve autonomous agents, whether representing human users or AI components it is usually of interest *who* can direct its evolution a particular way.

ATL* [3] extends temporal logics with *strategic modalities* that allow for reasoning about such properties. The operator $\langle\langle A \rangle\rangle \gamma$ says that agents in group (coalition) A have a *strategy* to enforce property γ . That is, as long as agents in A select events according to the strategy, γ will hold no matter what the other agents do. **ATL*** has been one of the most important and popular agent logics in the last two decades.

Definition 3 (Syntax of ATL*) *The language of **ATL*** is defined by the grammar:*

$$\begin{aligned} \varphi &::= p \mid \neg \varphi \mid \varphi \wedge \varphi \mid \langle\langle A \rangle\rangle \gamma, \\ \gamma &::= \varphi \mid \neg \gamma \mid \gamma \wedge \gamma \mid X \gamma \mid \gamma U \gamma, \end{aligned}$$

where $p \in PV$ and $A \subseteq \mathcal{A}$. The definitions of Boolean connectives and temporal operators X (“next”) and U (“strong until”) are standard; remaining operators R (“release”), G (“always”), and F (“sometime”) can be derived as usual.

Various types of strategies can be defined, based on the state information and memory of past states available to agents [27]. In this work, we focus on *imperfect information, imperfect recall strategies*.

Definition 4 (Strategy) A memoryless imperfect information strategy for agent $i \in \mathcal{A}$ is a function $\sigma_i: L_i \rightarrow 2^{Evt_i} \setminus \emptyset$ such that $\sigma_i(l) \in R_i(l)$ for each local state $l \in L_i$. A joint strategy σ_A of coalition $A \subseteq \mathcal{A}$ is a tuple of strategies σ_i , one for each agent $i \in A$.

The outcome set of a strategy collects all paths consistent with it, i.e., that may occur when the coalition follows the chosen strategy, while opposing agents choose freely from their protocols.

Definition 5 (Outcome) The outcome of strategy σ_A in global state $q \in S$ of model M , denoted by $out_M(q, \sigma_A)$, is the set of all paths $\pi = q_0 e_0 q_1 e_1 \dots$, such that $\pi \in out_M(q, \sigma_A)$ iff $q_0 = q$, and for each $j \geq 0$

$$\begin{cases} e_j \in \sigma_A(q_j^i) & \text{for every agent } i \in \text{Agent}(e_j) \cap A, \\ e_j \in \bigcup R_i(q_j^i) & \text{for every agent } i \in \text{Agent}(e_j) \setminus A, \end{cases}$$

where q^i denotes the local component l_i of q .

Definition 6 (Asynchronous semantics of ATL* [19]) The asynchronous semantics of the strategic modality in ATL^* is defined by the following clause:

$M, q \models \langle\langle A \rangle\rangle \gamma$ iff there is a strategy σ_A such that $out_M(q, \sigma_A) \neq \emptyset$ and, for each path $\pi \in out_M(q, \sigma_A)$, we have $M, \pi \models \gamma$.

The remaining clauses for temporal operators and Boolean connectives are standard, see [15].

3 Strategic Ability in Stochastic MAS

We start by recalling the basic definitions of stochastic multi-agent models and strategic play [7, 12, 17]. In our presentation, we follow mainly [5].

3.1 Probabilistic Models for MAS

Fix finite non-empty sets \mathbb{Agt} of agents a, a', \dots ; Act of actions α, α', \dots ; and PV of atomic propositions p, p', \dots . We write \mathbf{o} for a tuple $(o_a)_{a \in \mathbb{Agt}}$ of objects, one for each agent; such tuples are called *profiles*. A *joint action* or *move* α is an element of $Act^{\mathbb{Agt}}$. Given a profile \mathbf{o} and $C \subseteq \mathbb{Agt}$, we let o_C be the components for the agents in C . Moreover, we use \mathbb{Agt}_{-C} as a shorthand for $\mathbb{Agt} \setminus C$.

Distributions. Let X be a finite non-empty set. A (*probability*) *distribution* over X is a function $d : X \rightarrow [0, 1]$ such that $\sum_{x \in X} d(x) = 1$. $\text{Dist}(X)$ is the set of distributions over X . We write $x \in d$ for $d(x) > 0$. If $d(x) = 1$ for some element $x \in X$, then d is a *point* (a.k.a. *Dirac*) *distribution*. If d_i is a distribution over X_i , then, writing $X = \prod_i X_i$, the *product distribution* of the d_i is the distribution $d : X \rightarrow [0, 1]$ defined by $d(x) = \prod_i d_i(x_i)$.

Markov Chains. A *Markov chain* M is a tuple (S, d) where S is a set of states and $d \in \text{Dist}(S \times S)$ is a distribution. The values $d(s, t)$ are called *transition probabilities* of M .

Stochastic Concurrent Game Structures. A *stochastic concurrent game structure with imperfect information* (or simply *iCGS*) M is a tuple $(S, R, o, V, \{\sim\}_{a \in \mathbb{Agt}})$ where (i) S is a finite, non-empty set of *states*; (ii) $R : S \times \mathbb{Agt} \rightarrow 2^{Act} \setminus \{\emptyset\}$ is a function defining the available actions for each agent in each state, i.e., the repertoires of choices. We write $R(q)$ for the set of tuples $(R(q, a))_{a \in \mathbb{Agt}}$. It is usually assumed that $R(q, a) = R(q', a)$ whenever $q \sim_a q'$ (see below); (iii) for each state $q \in S$ and each move $\alpha \in R(q)$, the *stochastic transition function* o gives the (conditional) probability $o(q, \alpha)$ of a transition from state q for all $q' \in S$ if each player $a \in \mathbb{Agt}$ plays the action α_a ; we also write this probability as $o(q, \alpha)(q')$ to emphasize that $o(q, \alpha)$ is a probability distribution on S ; (iv) $V : S \rightarrow 2^{PV}$ is a *labelling function*; (v) $\sim \subseteq S \times S$ is an equivalence relation called the *observation relation* of agent a .

A pointed **CGS** is a pair (M, q) where $q \in S$ is a special state designed as initial. Throughout this paper, we assume that iCGSs are *uniform*, that is, if two states are indistinguishable for an agent a , then a has the same available actions in both states. Formally, if $q \sim q'$ then $R(q, a) = R(q', a)$, for any $q, q' \in S$ and $a \in \mathbb{Agt}$. For each state $q \in S$ and joint action $\alpha \in R(q)$, we also assume that there is a state $q' \in S$ such that $o(q, \alpha)(q')$ is non-zero, that is, every state has a successor state from a legal move.

Finally, we say that M is *deterministic* (instead of stochastic) if every $o(q, \alpha)$ is a point distribution.

Plays. A *play* in a iCGS M is an infinite sequence $\lambda = q_0 q_1 \dots$ of states such that there exists a sequence $\alpha_0 \alpha_1 \dots$ of joint-actions such that for every $i \geq 0$,

$\alpha_i \in R(q_i)$ and $q_{i+1} \in o(q_i, \alpha_i)$ (i.e., $o(q_i, \alpha_i)(q_{i+1}) > 0$). We write λ_i for state q_i , $\lambda_{\geq i}$ for the suffix of λ starting at position i . Finite prefixes of plays are called *histories*, and the set of all histories is denoted Hist . Write $\text{last}(h)$ for the last state of a history h .

Strategies. A (general) *probabilistic strategy* for agent $a \in \text{Agt}$ is a function $\sigma_a : \text{Hist} \rightarrow \text{Dist}(\text{Act})$ that maps each history to a probability distribution over the agent's actions. It is required that $\sigma_a(h)(\alpha) = 0$ if $\alpha \notin R(\text{last}(h), a)$. We denote the set of a 's general strategies by Str_a .

A *memoryless uniform probabilistic strategy* for an agent a is a function $\sigma_a : S \rightarrow \text{Dist}(\text{Act})$, in which: (i) for each q , we have $\sigma_a(q)(\alpha) = 0$ if $\alpha \notin R(q, a)$; and (ii) for all positions q, q' such that $q \sim q'$, we have $\sigma_a(q) = \sigma_a(q')$. We let Str_a be the set of memoryless uniform strategies for agent a . We call a memoryless strategy σ_a *deterministic* if $\sigma_a(q)$ is a point distribution for every q .

A *collective strategy* for agents $A \subseteq \text{Agt}$ is a tuple of strategies σ_a , one per agent $a \in A$. We denote the set of A 's collective general strategies and memoryless uniform strategies, respectively, by Str_A and Str_A^r . Moreover, a *strategy profile* is a tuple $\sigma = \sigma_{\text{Agt}}$ of strategies for all the agents. We write σ_a for the strategy of a in profile σ .

3.2 Probabilistic ATL and ATL*

Now we present the syntax and semantics of the Probabilistic Alternating-time Temporal Logics **PATL*** and **PATL** [4, 5, 12, 17], interpreted under the assumption of imperfect information. Again, we follow [5] in our presentation. Note that [5] adopts the *objective* semantics of strategic ability, where the coalition is supposed to have a strategy that works from the initial state of the game. In contrast, [17] uses the *subjective* semantics of strategic ability, where the agents need a strategy that wins from all the observationally equivalent states.¹ In this paper, we consider both accounts, as they are equally relevant in the literature. In particular, we integrate the *objective* and *subjective* semantics of probabilistic ability into a single framework.

Definition 7 (PATL*) *State formulas φ and path formulas ψ are defined by the following grammar, where $p \in \text{PV}$, $C \subseteq \text{Agt}$, d is a rational constant in $[0, 1]$, and $\bowtie \in \{\leq, <, >, \geq\}$:*

$$\varphi ::= p \mid \neg\varphi \mid \varphi \vee \varphi \mid \langle\langle C \rangle\rangle^{\bowtie d} \psi \quad (1)$$

$$\psi ::= \varphi \mid \neg\psi \mid \psi \vee \psi \mid X\psi \mid \psi U \psi \mid \psi R \psi \quad (2)$$

Formulas in PATL are all and only the state formulas φ .*

¹For a more thorough discussion of objective vs. subjective ability, cf. [1, 9].

An important syntactic restriction of **PATL**^{*}, namely **PATL**, is obtained by restricting path formulas as follows:

$$\psi ::= X\varphi \mid \varphi U\varphi \mid \varphi R\varphi \quad (3)$$

which is tantamount to the following grammar for state formulas:

$$\varphi ::= p \mid \neg\varphi \mid \varphi \vee \varphi \mid \langle\langle C \rangle\rangle^{\bowtie d} X\varphi \mid \langle\langle C \rangle\rangle^{\bowtie d} (\varphi U\varphi) \mid \langle\langle C \rangle\rangle^{\bowtie d} (\varphi R\varphi) \quad (4)$$

where again $p \in PV$, $C \subseteq \mathbb{Agt}$, and $\bowtie \in \{\leq, <, >, \geq\}$.

Formulas of **PATL** and **PATL**^{*} are interpreted over iCGSs.

Probability Space on Outcomes. An *outcome* of a strategy σ_A and a state q is a set of probability distributions over infinite paths, defined as follows.

First, by an *outcome path of a strategy profile σ and state q* , we refer to every play λ that starts with q and is extended by letting each agent follow their strategies in σ , i.e., $\lambda_0 = q$, and for every $k \geq 0$ there exists $\alpha_k \in \sigma(\lambda_k)$ such that $\lambda_{k+1} \in o(\lambda_k, \alpha_k)$. The set of outcome paths of strategy profile σ and state q is denoted as $outpaths(\sigma, q)$. A given iCGS M , strategy profile σ , and state q induce an infinite-state Markov chain $M_{\sigma, q}$ whose states are the finite prefixes of plays in $outpaths(\sigma, q)$. Such finite prefixes of plays are actually *histories*. Transition probabilities in $M_{\sigma, q}$ are defined as $p(h, hq') = \sum_{\alpha \in \text{Act}^{\mathbb{Agt}}} \sigma(h)(\alpha) \cdot o(\text{last}(h), \alpha)(q')$. The Markov chain $M_{\sigma, q}$ induces a canonical probability space on its set of infinite paths [22], and thus also on $outpaths(\sigma, q)$.²

Given a coalitional strategy $\sigma_C \in \prod_{a \in C} \text{Str}_a$, we define its *objective outcome* from state $q \in S$ as the set $out_{o, C}(\sigma_C, q) = \{out((\sigma_C, \sigma_{\mathbb{Agt} \setminus C}), q) \mid \sigma_{\mathbb{Agt} \setminus C} \in \text{Str}_{\mathbb{Agt} \setminus C}\}$ of probability measures consistent with strategy σ_C of the players in C . Note that the opponents can use any general strategy for $\sigma_{\mathbb{Agt} \setminus C}$, even if C must employ only uniform memoryless strategies for σ_C .

The *subjective outcomes* are then defined as the set

$$out_{s, C}(\sigma_C, q) = \bigcup_{q' \sim_a q, a \in C} out_{o, C}(\sigma_C, q') \quad (5)$$

We will use $\mu_{x, q}^{\sigma_C}$ to range over the elements of $out_{x, C}(\sigma_C, q)$, for $x \in \{s, o\}$.

Semantics. For x equal to either s or o , state and path formulas in **PATL**^{*} are interpreted in a iCGS M and a state q , resp. path λ , according to the x -interpretation of strategy operators, as follows (clauses for Boolean connectives are omitted as immediate):

$$M, q \models_x p \quad \text{iff } p \in V(q)$$

²This is a classical construction, see for instance [6, 13].

$M, q \models_x \langle\langle C \rangle\rangle^{\bowtie d} \psi$	iff $\exists \sigma_C \in \prod_{a \in C} Str_a$ such that $\forall \mu_{x,q}^{\sigma_C} \in out_{x,C}(\sigma_C, q),$ $\mu_{x,s}^{\sigma_C}(\{\lambda \mid M, \lambda \models_x \psi\}) \bowtie d$
$M, \lambda \models_x X \psi$	iff $M, \lambda_{\geq 1} \models_x \psi$
$M, \lambda \models_x \psi_1 U \psi_2$	iff $\exists k \geq 0$ s.t. $M, \lambda_{\geq k} \models_x \psi_2$ and $\forall j \in [0, k) M, \lambda_{\geq j} \models_x \psi_1$
$M, \lambda \models_x \psi_1 R \psi_2$	iff $\forall k \geq 0, M, \lambda_{\geq k} \models_x \psi_2$ or $\exists j \in [0, k) \text{ s.t. } M, \lambda_{\geq j} \models_x \psi_1$

Remark 1 Note that standard **ATL**^{*} formulas $\langle\langle C \rangle\rangle \psi$ can be interpreted in stochastic iCGS by simply ignoring the probabilities of transitions, i.e., via a projection of the probabilistic transition relation o to the non-probabilistic relation T defined by $(q, \alpha, q') \in T$ iff $o(q, \alpha)(q') > 0$.

Remark 2 Moreover, the logic of Probabilistic CTL^{*} (**PCTL**^{*}) can be embedded in **PATL**^{*} by assuming $P^{\bowtie d} \psi \equiv \langle\langle \emptyset \rangle\rangle^{\bowtie d} \psi$.

4 Case Study: Perun Ballistic Rocket by SpaceForest

This section provides an overview of the Perun ballistic rocket developed by SpaceForest, a Polish technology company specializing in rocket technologies and space systems. We describe the company's background, the technical specifications of the Perun rocket, its payload section designed for scientific experiments, and the research applications it supports.

4.1 Company Background

SpaceForest is a Polish technology company headquartered in Gdynia, specializing in rocket technologies, radars and SAR (Synthetic Aperture Radar), advanced electronics, microwave filters, and composites. Founded in 2004, the company has accumulated 21 years of experience in space technologies, with over 50 dedicated employees (95% of the team consists of technically qualified personnel). Its business profile spans the space, aviation, defense industries, and advanced electronic and material technologies.

Table 1: Basic technical parameters of the PERUN rocket

Parameter	Value
Height	11.5m
Diameter	0.45m
Launch mass	970kg
Apogee	150km
Time in space	approx. 5min
Payload capacity	50kg
Internal payload bay diameter	444mm
Internal payload bay length	830mm
Propulsion type	Eco-friendly rocket engine

4.2 Technical Specifications

The PERUN rocket is a two-stage, hybrid engine (solid fuel and liquid oxidizer) suborbital vehicle designed to carry scientific and technological payloads to altitudes of up to 150km. It features a recoverable payload section, advanced telemetry and control systems, and a low acceleration profile suitable for sensitive experiments. Technical specifications of the PERUN rocket are summarized in Table 1.

Key Systems and Technologies The PERUN rocket incorporates several advanced systems and technologies to ensure mission success and safety:

- **Telecommunication system:** Two-way real-time data transmission with in-flight mission parameter modification capability
- **Thrust vector control (VTC) system:** Precision engine thrust management for optimal flight trajectory
- **Telemetry and control:** Comprehensive flight parameter monitoring and remote command system
- **Recoverable payload section:** Engineered for safe payload return to Earth
- **Low acceleration profile:** Optimized launch conditions for sensitive experimental payloads

4.3 Payload Section and Experiment Integration

The PERUN rocket's payload section is specifically designed to support a variety of scientific and technological experiments in microgravity conditions.

Payload Section Parameters

- Nominal payload mass: 50kg
- Research altitude: 150km
- Microgravity duration: approx. 5min
- Maximum payload dimensions: 830mm length × 444mm diameter
- Payload types supported: Active or passive experimental configurations

Integration Process

- Mission-specific payload adaptation and qualification
- Late access capability to payload section prior to launch
- Clean room handling environment (ISO 7 class)
- Flexible launch options from designated terrestrial locations

4.4 Research Applications

The PERUN rocket's payload section is designed to accommodate a wide range of scientific and technological experiments, enabling researchers to explore various phenomena in microgravity.

Scientific Research Domains

- **Life sciences and medicine:** Cellular and tissue behavior in microgravity; pharmaceutical validation
- **Human physiology:** Neural and immune cell response to weightlessness simulation
- **Chemistry:** Convection-free reaction analysis; crystallization kinetics studies

- **Physics:** Fundamental theory verification in weightlessness and high-acceleration environments
- **Fluid dynamics and combustion:** Liquid/gas behavior and fire propagation in microgravity
- **Materials science:** Crystallization processes and novel material properties in zero-gravity

Technological Validation Applications

- Pre-orbital validation of electronic components, sensors, and mechanical systems
- Space construction techniques: Assembly methods and robotics testing in weightlessness
- Upper atmospheric research: Data collection from regions inaccessible to balloons and drones
- Astronomical instrumentation: Testing optical systems above atmospheric interference

4.5 Mission Timeline and Development

The PERUN rocket is currently in the advanced testing phase, with a series of planned test flights and a roadmap for operational deployment.

Test Flight Schedule (2025-2026)

- October 2025: Ustka test flight (90% payload capacity utilization)
- November 2025: Ustka test flight (75% payload capacity utilization)
- First half 2026: Portuguese test flight (50% payload capacity utilization)
- Second half 2026: Danish sea platform test flight (45% payload capacity utilization)

Operational Development Path

- 2026-2027: Commercialization phase with payload reservations and exclusive mission offerings
- 2026-2027: Implementation of land recovery systems
- 2026-2027: Pursuit of Polish spaceport access or foreign launch site agreements
- Post-2027: Development of enhanced PERUN variant for 300km altitude operations

4.6 Representative Research Missions

Below are selected experiments planned for the PERUN rocket's payload section, showcasing its scientific and technological capabilities.

MXene in LEO (AGH University of Science and Technology) Testing six MXene-based sensors to evaluate material response to suborbital flight conditions (thermal variations, vibrations, pressure changes) under Prof. Tadeusz Uhl's leadership.

THOR (Analog Astronaut Training Center) Investigation of acceleration effects on biological growth media under Dr. Agata Kołodziejczyk, utilizing PERUN's late-access capability for biotechnology applications.

AstroFarms Microgravity analysis of symbiotic bacterial-yeast cultures (SCOBY) examining survivability, cellulose production, metabolic changes, and potential space applications of kombucha fermentation.

Lab-on-a-Chip World-first experiment with living bone cells on microfluidic platform assessing technology resilience to launch stresses and cellular survival in flight conditions.

Toraf Germination analysis of seeds exposed to suborbital conditions (extreme cold, radiation, low pressure) compared with terrestrial control samples.

5 6-DOF Rocket Flight Simulator: Technical Description and Capabilities

The 6-DOF (Six Degrees of Freedom) Rocket Flight Simulator is an in-house developed simulation environment created by SpaceForest for high-fidelity modeling and analysis of sounding rocket trajectories, dynamics, and control systems. This comprehensive simulation platform has been validated against actual SpaceForest flight data, providing reliable prediction capabilities throughout the entire mission profile from launch through recovery.

5.1 Simulation Architecture

The simulator is built using a modular architecture that allows for flexible configuration of vehicle parameters, environmental conditions, and mission profiles. It integrates various physical models, numerical solvers, and data processing tools to accurately replicate the complex interactions affecting rocket flight.

- **Six Degrees of Freedom Model:** Complete dynamic model resolving translational motion (position, velocity, acceleration) and rotational motion (attitude, angular rates, angular acceleration)
- **Coordinate Systems:** Multiple reference frames including inertial, body-fixed, wind reference, and geodetic coordinate systems
- **Physical Models:**
 - *Propulsion System:* Thrust magnitude and direction, propellant mass depletion, Thrust Vector Control (TVC) dynamics, motor performance characteristics
 - *Aerodynamics:* Force and moment coefficients, Mach number and angle of attack dependencies, center of pressure modeling, atmospheric density variation
 - *Environmental Models:* Atmospheric conditions (temperature, pressure, density), gravitational field modeling, wind models (steady, gusts, turbulence)

5.2 Mission Event Modeling

The simulator includes detailed event modeling capabilities to replicate critical mission phases and transitions:

- **Stage Separation:**

- Payload-booster separation mechanics
- Separation impulse modeling
- Post-separation trajectory divergence
- Independent tracking of separated components

- **Recovery System:**

- Multi-stage parachute deployment
- Drogue and main parachute sequencing
- Drag coefficient modeling
- Descent rate calculations
- Touchdown condition prediction

5.3 Sensor Simulation Capabilities

The simulator incorporates realistic sensor models to generate synthetic measurements for onboard navigation and control systems:

- **IMU Simulation:**

- 3-axis accelerometer and gyroscope modeling
- Measurement noise (white noise, random walk)
- Bias instability and scale factor errors
- Sensor misalignment errors
- Saturation limits

- **GPS Receiver Simulation:**

- Realistic accuracy characteristics
- Variable update rate modeling
- Signal obstruction scenarios

5.4 Control System Development Environment

The simulator provides a robust environment for developing and testing rocket guidance, navigation, and control (GNC) algorithms:

- Trajectory design and optimization tools
- Guidance algorithm implementation framework
- Attitude control system design capabilities
- Thrust vector control algorithm development
- Stability augmentation system modeling
- Control law design and gain tuning interfaces
- Stability analysis across the complete flight envelope

5.5 Software-in-the-Loop (SIL) Capabilities

The simulator supports Software-in-the-Loop testing, enabling integration of actual flight software with the simulation environment:

- Real-time or faster-than-real-time simulation execution
- Complete closed-loop vehicle and control integration
- Flight software reads simulated sensor data as if from actual hardware
- Control algorithms compute actuator commands based on simulated conditions
- Iterative execution through entire mission profile
- Automated test case execution framework
- Monte Carlo simulation for statistical analysis
- Fault injection and failure mode testing scenarios
- Regression testing capabilities for software updates

5.6 Validation and Verification

The simulator has undergone extensive validation against actual SpaceForest flight data to ensure accuracy and reliability:

- Extensive validation against SpaceForest flight data
- Trajectory reconstruction from telemetry comparisons
- Model parameter tuning based on flight measurements
- Position, velocity, and attitude accuracy validation
- Event timing correlation (separation, parachute deployment)
- Descent rate and landing location prediction verification
- Continuous improvement through iterative flight data integration

5.7 Primary Applications

The 6-DOF Rocket Flight Simulator serves as a critical tool throughout the rocket development lifecycle:

- Mission design and trajectory optimization
- Control system development and validation
- Flight software verification through SIL testing
- Monte Carlo analysis for comprehensive risk assessment
- Sensitivity studies and parametric analysis
- Post-flight analysis and correlation with mission data
- Pre-flight mission rehearsal and verification
- Crew training and procedure validation

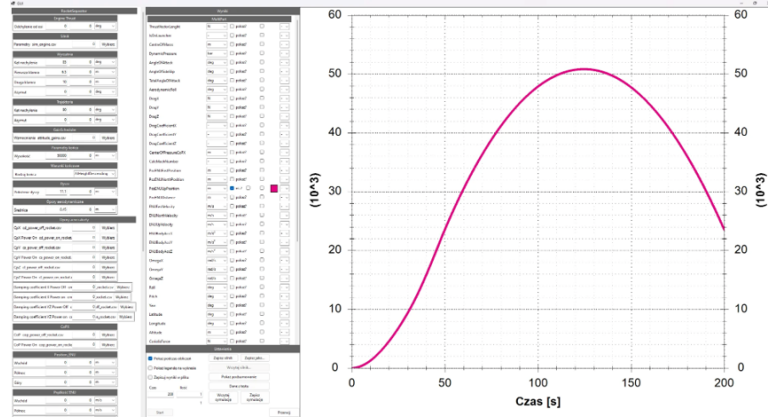


Figure 1: High-fidelity simulator architecture and sample output used to generate synthetic rocket trajectories.

5.8 Operational Implementation

The simulator has been successfully integrated into SpaceForest's development workflow, supporting multiple rocket development programs including the PERUN suborbital vehicle. Its modular architecture allows for configuration specific to different vehicle types while maintaining core simulation capabilities. The system supports both interactive simulation sessions for design exploration and automated batch processing for comprehensive parameter studies.

Figure 1 illustrates the simulator components and example outputs referenced in the simulator and data sources description.

6 Formal Modelling of a Rocket

Our verification framework models the ballistic rocket system as a **probabilistic state transition system** $\mathcal{M} = (S, s_0, Act, P, L)$ where:

- S is the set of states representing rocket configurations at discrete time steps
- $s_0 \in S$ is the initial launch state
- $Act = \{\text{continue, disengage}\}$ is the action set (engine continuation or disengagement)
- $P : S \times Act \times S \rightarrow [0, 1]$ defines probabilistic state transitions
- $L : S \rightarrow 2^{AP}$ labels states with atomic propositions

6.1 State Representation

Each state $s \in S$ encapsulates the rocket's physical configuration at time t (seconds since launch) as a tuple:

$$s = \langle t, v, p, \theta, \phi, \psi \rangle$$

where:

- $v \in \mathbb{R}^3$ is the 3D velocity vector (m/s) from inertial measurement units
- $p = (lat, lon, alt) \in \mathbb{R}^3$ is the GPS position
- $\theta = \text{pitch angle (rad)}, \phi = \text{roll angle (rad)}, \psi = \text{yaw angle (rad)}$ from attitude sensors

We compare each observed state to a corresponding reference (ideal) state at the same time using a single deviation score that combines position, velocity, and attitude differences. States are classified by thresholding this deviation: a GoodState means the deviation is below a design-specified "good" threshold, and a BadState means the deviation exceeds a larger, design-specified "bad" threshold. Threshold values are chosen as design parameters (for example, the good threshold may correspond to a position-equivalent deviation of about 500m). These classifications depend only on the instantaneous, time-aligned deviation and do not rely on landing-probability estimates.

6.2 Data Acquisition and Model Construction

The transition probabilities P are derived from two complementary data sources:

1. **Historical test flights:** launches providing real-world trajectory data under documented weather conditions
2. **High-fidelity simulator:** Company-developed computational simulation model that generates synthetic trajectories under randomized atmospheric conditions:
 - Weather parameters sampled from historical distributions
 - simulated trajectories covering edge cases beyond test flight capabilities
 - Simulator validated against test flight data

All sensor data is time-synchronized and discretized into k -second intervals to create state sequences $\{s_0, s_1, \dots, s_T\}$, where k is a design parameter of the model.

6.3 Probabilistic Transition Modeling

Transition probabilities are empirically derived through **frequentist counting** over the combined dataset:

$$P(s, a, s') = \frac{N(s, a, s')}{\sum_{s'' \in S} N(s, a, s'')}$$

where $N(s, a, s')$ counts occurrences of transition $s \xrightarrow{a} s'$ across all trajectories.

7 Results and Analysis

We have created three distinct models of the rocket system:

- **Model A:** perfect information model without probabilistic transitions (non-deterministic)
- **Model B:** perfect information model with probabilistic transitions derived from the simulator data
- **Model C:** imperfect information model with probabilistic transitions, where the rocket has only partial observability of its state (e.g., noisy sensor readings), and can read only integer approximations from sensors, introducing uncertainty in state estimation

Classes of models are defined according to the time precision parameter. Since data from the simulator and test flights is recorded at 0.001s intervals, we aggregate states into coarser time steps of 1.0s, 0.5s, 0.2s, and 0.1s to create models of varying granularity. Finer time precision leads to larger state spaces and more detailed transition dynamics.

Top portions of the state transition diagrams for Models A and B at time precision of 3.0s are shown in Figures 3 and 4, respectively. These diagrams illustrate the branching structure of possible rocket states and transitions over time.

Example state transition diagrams for Model A at time precision of 6.0s is shown in Figure 2. As the time precision increases, the number of states and transitions grows significantly, capturing more nuanced rocket behavior.

We specify critical safety properties using PATL formulas to identify states where the rocket deviates from the desired trajectory and risks landing in restricted areas. We define several key properties. We verified these properties on all three models using the STV model checker. For Model A we used the standard ATL model checking approach, while for Models B and C we employed the probabilistic extension of ATL (PATL) to account for stochastic transitions. In all cases we set

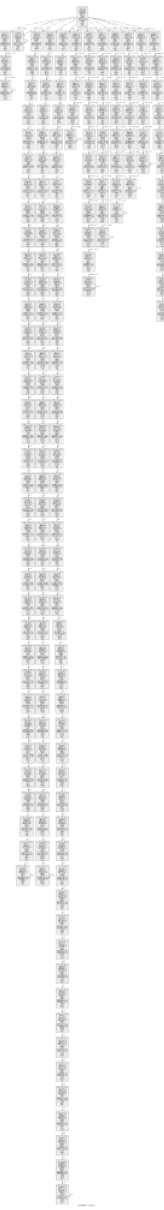


Figure 2: Model A state transition diagram for time precision 6.0s (simplified for illustration)

three probability thresholds: $p = 0.9$ for high-confidence properties, $p = 0.5$ for moderate-confidence properties and $p = 0.25$ for low-confidence properties.

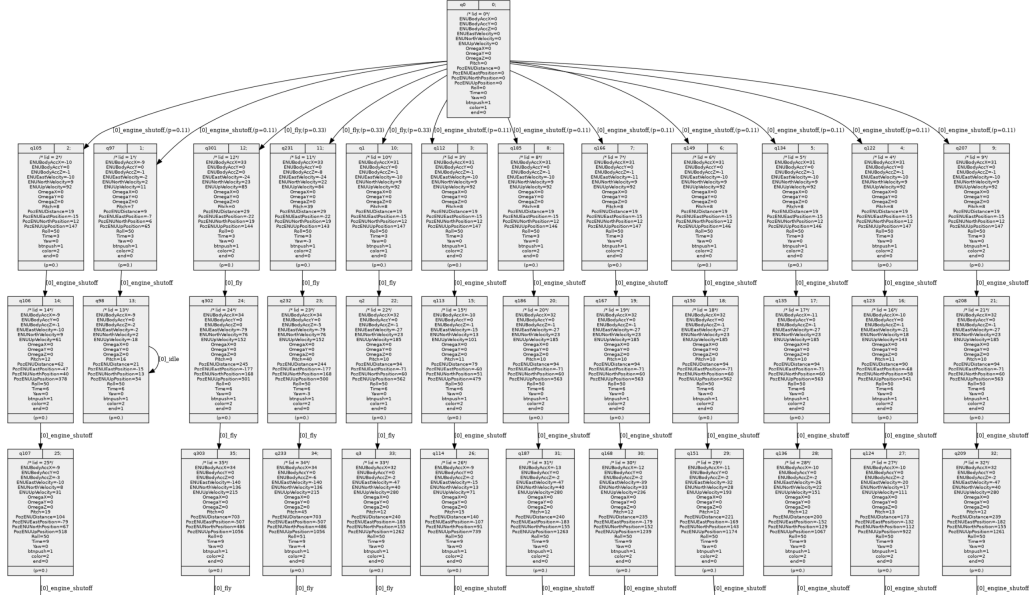


Figure 3: Top part of the Model A state transition diagram for time precision 3.0s (simplified for illustration)

In all of our experiments the platform for model checking was a machine with an AMD Ryzen 7 5700X3D CPU @ 3.0GHz and 64GB of RAM. All times are given in seconds. Timeout was set to 4 hours.

7.1 Property 1: Eventual Good State and Finish

For model A we verify that the rocket can eventually reach a good state and complete the mission:

$$\varphi_1 = \langle \langle \text{Rocket} \rangle \rangle \mathbf{F}(\text{GoodState} \wedge \text{Finish})$$

For models B and C we verify that the rocket can eventually reach a good state and complete the mission with at least probability p :

$$\varphi_{1p} = \langle \langle \text{Rocket} \rangle \rangle^{\geq p} \mathbf{F}(\text{GoodState} \wedge \text{Finish})$$

Model A Results Results for Model A are summarized in Table 2. The model generation time, verification time, and verification result (TRUE/FALSE) are reported for each time precision. As we can observe the size of the model increases linearly with finer time precision, but verification remains efficient. The formula was verified as TRUE in all cases.

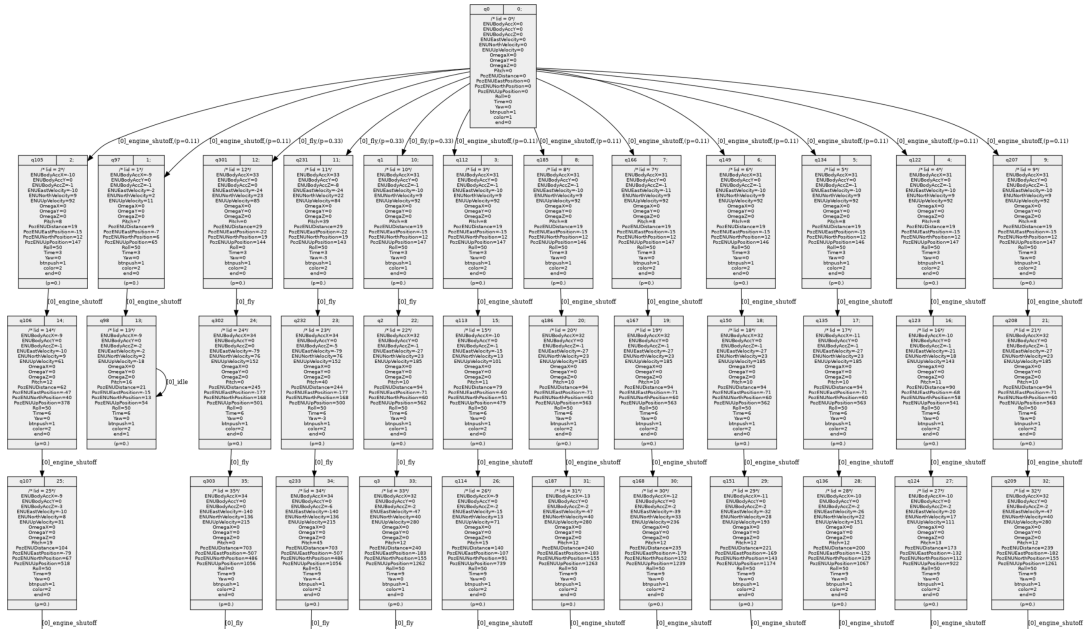


Figure 4: Top part of the Model B state transition diagram for time precision 3.0s (simplified for illustration)

Model B Results Results for Model B are summarized in Table 3. For each time precision, we report the number of states, model generation time, verification time, and verification result for probability thresholds $p = 0.25$, $p = 0.5$, and $p = 0.9$. As we can see, verification times increase significantly with finer time precision, and the property is verified as TRUE at $p = 0.25$ and also at $p = 0.5$ but only for the coarsest model. For higher precision models we reach timeout for the verification.

Model C Results Results for Model C are summarized in Table 4. For each time precision, we report the number of states, model generation time, verification time, and verification result for probability thresholds $p = 0.25$, $p = 0.5$, and $p = 0.9$. As we can see, verification times increase significantly with finer time precision, and the property is verified as TRUE only at $p = 0.25$. Similarly to Model B, for higher precision models we reach timeout for the verification.

7.2 Property 2: Disengagement Safety

For model A we verify that if the rocket disengages, it will remain in a good state:

time precision	#states	model gen. time	verif. time	verif. result
1.0	1102	0.102	0.008	TRUE
0.5	2209	0.213	0.023	TRUE
0.2	5602	0.801	0.089	TRUE
0.1	11210	2.370	0.119	TRUE

Table 2: Model A verification results for Property 1 at varying time precisions.

time precision	#states	m. gen. time	p=0.25		p=0.5		p=0.9	
			v. time	v. result	v. time	v. result	v. time	v. result
1.0	1102	0.099	4.482	TRUE	4.636	TRUE	6.183	FALSE
0.5	2209	0.216	59.652	TRUE	76.702	FALSE	76.659	FALSE
0.2	5602	0.801	1022.352	TRUE	1350.994	FALSE	1643.021	FALSE
0.1	11210	2.388	timeout	-	timeout	-	timeout	-

Table 3: Model B verification results for Property 1 at varying time precisions.

$$\varphi_2 = \langle\langle \text{Rocket} \rangle\rangle \mathbf{G}(\text{Disengaged} \implies \text{GoodState})$$

For models B and C we verify that if the rocket disengages, it will remain in a good state with at least probability p :

$$\varphi_{2p} = \langle\langle \text{Rocket} \rangle\rangle^{\geq p} \mathbf{G}(\text{Disengaged} \implies \text{GoodState})$$

Model A Results Results for Model A are summarized in Table 5. The model generation time, verification time, and verification result (TRUE/FALSE) are reported for each time precision. The formula was verified as TRUE in all cases.

Model B Results Results for Model B are summarized in Table 6. For each time precision, we report the number of states, model generation time, verification time, and verification result for three probability thresholds $p = 0.25$, $p = 0.5$, and $p = 0.9$. As we can see, verification times increase with finer time precision, and

time precision	#states	m. gen. time	p=0.25		p=0.5		p=0.9	
			v. time	v. result	v. time	v. result	v. time	v. result
1.0	1102	0.099	6.470	TRUE	6.861	FALSE	9.377	FALSE
0.5	2209	0.216	80.493	TRUE	95.028	FALSE	96.904	FALSE
0.2	5602	0.801	1801.057	TRUE	2061.072	FALSE	2106.082	FALSE
0.1	11210	2.388	timeout	-	timeout	-	timeout	-

Table 4: Model C verification results for Property 1 at varying time precisions.

time precision	#states	model gen. time	verif. time	verif. result
1.0	1102	0.102	0.007	TRUE
0.5	2209	0.213	0.011	TRUE
0.2	5602	0.801	0.028	TRUE
0.1	11210	2.370	0.077	TRUE

Table 5: Model A verification results for Property 2 at varying time precisions.

time precision	#states	m. gen. time	p=0.25		p=0.5		p=0.9	
			v. time	v. result	v. time	v. result	v. time	v. result
1.0	1102	0.099	0.370	TRUE	0.359	TRUE	0.810	FALSE
0.5	2209	0.216	1.772	TRUE	6.709	FALSE	6.768	FALSE
0.2	5602	0.801	17.243	TRUE	16.651	TRUE	166.987	FALSE
0.1	11210	2.388	1978.696	TRUE	3659.402	FALSE	3649.928	FALSE

Table 6: Model B verification results for Property 2 at varying time precisions.

the property is verified as TRUE only for lower probability thresholds.

Model C Results Results for Model C are summarized in Table 7. For each time precision, we report the number of states, model generation time, verification time, and verification result for three probability thresholds $p = 0.25$, $p = 0.5$, and $p = 0.9$. As we can see, verification times increase with finer time precision, and the property is verified as TRUE only for lower probability thresholds.

7.3 Property 3: Finish in Good or Disengaged State

For model A we verify that the rocket will finish the mission in either a good state or the engine will be disengaged:

$$\varphi_3 = \langle \langle \text{Rocket} \rangle \rangle \mathbf{G}(\text{Finish} \implies (\text{GoodState} \vee \text{Disengaged}))$$

time precision	#states	m. gen. time	p=0.25		p=0.5		p=0.9	
			v. time	v. result	v. time	v. result	v. time	v. result
1.0	1102	0.099	1.437	TRUE	1.593	FALSE	1.952	FALSE
0.5	2209	0.216	2.963	TRUE	9.342	FALSE	9.499	FALSE
0.2	5602	0.801	26.483	TRUE	28.592	FALSE	304.063	FALSE
0.1	11210	2.388	2673.982	TRUE	4203.124	FALSE	4381.327	FALSE

Table 7: Model C verification results for Property 2 at varying time precisions.

For models B and C we verify that the rocket will finish the mission in either a good state or the engine will be disengaged with at least probability p :

$$\varphi_{3p} = \langle\langle \text{Rocket} \rangle\rangle^{\geq p} \mathbf{G}(\text{Finish} \implies (\text{GoodState} \vee \text{Disengaged}))$$

time precision	#states	model gen. time	verif. time	verif. result
1.0	1102	0.102	0.013	TRUE
0.5	2209	0.213	0.001	TRUE
0.2	5602	0.801	0.006	TRUE
0.1	11210	2.370	0.008	TRUE

Table 8: Model A verification results for Property 3 at varying time precisions.

Model A Results Results for Model A are summarized in Table 8. The model generation time, verification time, and verification result (TRUE/FALSE) are reported for each time precision. The formula was verified as TRUE in all cases.

Model B Results Results for Model B are summarized in Table 9. For each time precision, we report the number of states, model generation time, verification time, and verification result for three probability thresholds $p = 0.25$, $p = 0.5$, and $p = 0.9$. As we can see, the property is verified as TRUE in all cases.

Model C Results Results for Model C are summarized in Table 10. For each time precision, we report the number of states, model generation time, verification time, and verification result for three probability thresholds $p = 0.25$, $p = 0.5$, and $p = 0.9$. As we can see, the property is verified as TRUE only for lower probability thresholds.

time precision	#states	m. gen. time	p=0.25		p=0.5		p=0.9	
			v. time	v. result	v. time	v. result	v. time	v. result
1.0	1102	0.099	0.208	TRUE	0.215	TRUE	0.218	TRUE
0.5	2209	0.216	1.015	TRUE	1.049	TRUE	1.392	TRUE
0.2	5602	0.801	6.586	TRUE	6.642	TRUE	6.543	TRUE
0.1	11210	2.388	29.146	TRUE	29.441	TRUE	29.758	TRUE

Table 9: Model B verification results for Property 3 at varying time precisions.

time precision	#states	m. gen. time	p=0.25		p=0.5		p=0.9	
			v. time	v. result	v. time	v. result	v. time	v. result
1.0	1102	0.099	0.881	TRUE	0.893	TRUE	0.899	FALSE
0.5	2209	0.216	2.594	TRUE	2.690	TRUE	3.527	FALSE
0.2	5602	0.801	9.720	TRUE	10.351	TRUE	10.550	FALSE
0.1	11210	2.388	42.038	TRUE	43.403	TRUE	43.602	FALSE

Table 10: Model C verification results for Property 3 at varying time precisions.

8 Conclusion and Future Work

This work has presented a comprehensive framework for formal verification of probabilistic multi-agent systems applied to ballistic rocket flight trajectories using Probabilistic Alternating-Time Temporal Logic (PATL). Our research bridges the gap between theoretical formal verification methods and practical aerospace engineering challenges, demonstrating how strategic reasoning can enhance safety assurance in critical systems.

The key contributions of this work include:

- Development of an innovative verification framework specifically designed for analyzing safety properties of ballistic rockets engineered to achieve microgravity conditions for scientific experimentation.
- Integration of authentic flight telemetry data with high-fidelity simulation to construct probabilistic state transition systems that rigorously account for environmental stochasticity, particularly meteorological variability.
- Formalization of mission-critical safety properties through PATL specifications that enable systematic identification of trajectory deviation states where rockets risk landing in prohibited or hazardous zones.
- Implementation of a practical verification approach validated against the Perun Rocket system developed by SpaceForest, demonstrating real-world applicability of advanced formal methods.
- Comparative analysis of three distinct modeling approaches (non-probabilistic, probabilistic with perfect information, and probabilistic with imperfect information) that reveals important trade-offs between model fidelity and verification feasibility.

Our experimental validation demonstrates that while deterministic models (Model A) consistently verify safety properties across all time precisions, probabilistic

models reveal critical limitations when higher confidence thresholds are required. These findings underscore the importance of appropriate confidence threshold selection when deploying formal verification in safety-critical aerospace applications. The verification results also highlight the computational challenges inherent in strategic ability verification for probabilistic systems with imperfect information. As time precision increases, both state space complexity and verification time grow significantly. This demonstrates the practical limitations of current model checking approaches when applied to high-fidelity aerospace systems.

Future work will focus on several promising directions. First of all, in order to reduce the state space explosion problem, we plan to develop efficient model reduction techniques specifically tailored for aerospace applications. Additionally, we aim to explore new verification algorithms that can better handle the complexities of probabilistic multi-agent systems with imperfect information such as fix-point approximations.

This research establishes a foundation for applying formal verification methods to commercial spaceflight systems, potentially setting new standards for safety assurance in the rapidly growing private space industry. By demonstrating the practical utility of PATL in analyzing real-world aerospace systems, we hope to encourage wider adoption of formal methods throughout the space technology sector, ultimately contributing to safer and more reliable access to space for scientific research and commercial applications.

Acknowledgements The work has been supported by NCBR Poland and FNR Luxembourg under the PolLux/FNR-CORE project SpaceVote (POLLUX-XI/14/SpaceVote/2023 and C22/IS/17232062/SpaceVote). For the purpose of open access, and in fulfilment of the grant agreement, the authors have applied CC BY 4.0 license to any Author Accepted Manuscript version arising from this submission.

References

- [1] T. Ågotnes, V. Goranko, W. Jamroga, and M. Wooldridge. Knowledge and ability. In H.P. van Ditmarsch, J.Y. Halpern, W. van der Hoek, and B.P. Kooi, editors, *Handbook of Epistemic Logic*, pages 543–589. College Publications, 2015.
- [2] R. Alur, T. Henzinger, F. Mang, S. Qadeer, S. Rajamani, and S. Tasiran. MOCHA: Modularity in model checking. In *Proceedings of Computer Aided Verification (CAV)*, volume 1427 of *Lecture Notes in Computer Science*, pages 521–525. Springer, 1998.

- [3] R. Alur, T. A. Henzinger, and O. Kupferman. Alternating-time Temporal Logic. *Journal of the ACM*, 49:672–713, 2002.
- [4] Francesco Belardinelli, Wojciech Jamroga, Munyque Mittelmann, and Aniello Murano. Strategic abilities of forgetful agents in stochastic environments. In *Proceedings of the 20th International Conference on Principles of Knowledge Representation and Reasoning, KR*, pages 726–731, 2023.
- [5] Francesco Belardinelli, Wojtek Jamroga, Munyque Mittelmann, and Aniello Murano. Verification of stochastic multi-agent systems with forgetful strategies. In *Proceedings of AAMAS*, pages 160–169. IFAAMAS/ACM, 2024.
- [6] Raphaël Berthon, Nathanaël Fijalkow, Emmanuel Filiot, Shibashis Guha, Bastien Maubert, Aniello Murano, Laureline Pinault, Sophie Pinchinat, Sasha Rubin, and Olivier Serre. Alternating tree automata with qualitative semantics. *ACM Trans. Comput. Logic*, 22(1):1–24, 2020.
- [7] Craig Boutilier. Sequential optimality and coordination in multiagent systems. In *Proceedings of International Joint Conference on Artificial Intelligence (IJCAI)*, pages 478–485, 1999.
- [8] N. Bulling, J. Dix, and W. Jamroga. Model checking logics of strategic ability: Complexity. In M. Dastani, K. Hindriks, and J.-J. Meyer, editors, *Specification and Verification of Multi-Agent Systems*, pages 125–159. Springer, 2010.
- [9] N. Bulling and W. Jamroga. Comparing variants of strategic ability: How uncertainty and memory influence general properties of games. *Journal of Autonomous Agents and Multi-Agent Systems*, 28(3):474–518, 2014.
- [10] S. Busard, C. Pecheur, H. Qu, and F. Raimondi. Reasoning about memoryless strategies under partial observability and unconditional fairness constraints. *Information and Computation*, 242:128–156, 2015.
- [11] Petr Cermák, Alessio Lomuscio, and Aniello Murano. Verifying and synthesising multi-agent systems against one-goal strategy logic specifications. In *Proceedings of AAAI*, pages 2038–2044, 2015.
- [12] Taolue Chen and Jian Lu. Probabilistic alternating-time temporal logic and model checking algorithm. In *Proceedings of FSKD, Volume 2*, pages 35–39. IEEE Computer Society, 2007.
- [13] E.M. Clarke, T.A. Henzinger, H. Veith, and R. Bloem, editors. *Handbook of Model Checking*. Springer, 2018.

- [14] C. Dima and F.L. Tiplea. Model-checking ATL under imperfect information and perfect recall semantics is undecidable. *CoRR*, abs/1102.4225, 2011.
- [15] E.A. Emerson. Temporal and modal logic. In J. van Leeuwen, editor, *Handbook of Theoretical Computer Science*, volume B, pages 995–1072. Elsevier, 1990.
- [16] D.P. Guelev, C. Dima, and C. Enea. An alternating-time temporal logic with knowledge, perfect recall and past: axiomatisation and model-checking. *Journal of Applied Non-Classical Logics*, 21(1):93–131, 2011.
- [17] X. Huang, K. Su, and C. Zhang. Probabilistic alternating-time temporal logic of incomplete information and synchronous perfect recall. In *Proceedings of AAAI-12*, 2012.
- [18] X. Huang and R. van der Meyden. Symbolic model checking epistemic strategy logic. In *Proceedings of AAAI Conference on Artificial Intelligence*, pages 1426–1432, 2014.
- [19] W. Jamroga, W. Penczek, T. Sidoruk, P. Dembiński, and A. Mazurkiewicz. Towards partial order reductions for strategic ability. *Journal of Artificial Intelligence Research*, 68:817–850, 2020.
- [20] Wojciech Jamroga, Yan Kim, Damian Kurpiewski, and Peter Y. A. Ryan. Towards model checking of voting protocols in uppaal. In *Proceedings of E-Vote-ID*, volume 12455 of *Lecture Notes in Computer Science*, pages 129–146. Springer, 2020.
- [21] Wojciech Jamroga, Michał Knapik, Damian Kurpiewski, and Łukasz Mikulski. Approximate verification of strategic abilities under imperfect information. *Artificial Intelligence*, 277, 2019.
- [22] John G Kemeny, J Laurie Snell, and Anthony W Knapp. Stochastic processes. In *Denumerable Markov Chains*, pages 40–57. Springer, 1976.
- [23] D. Kurpiewski and D. Marmsober. Strategic logics for collaborative embedded systems. specification and verification of collaborative embedded systems using strategic logics. In preparation, 2019.
- [24] Damian Kurpiewski, Witold Pazderski, Wojciech Jamroga, and Yan Kim. STV+Reductions: Towards practical verification of strategic ability using model reductions. In *Proceedings of AAMAS*, pages 1770–1772. ACM, 2021.

- [25] A. Lomuscio, H. Qu, and F. Raimondi. MCMAS: An open-source model checker for the verification of multi-agent systems. *International Journal on Software Tools for Technology Transfer*, 19(1):9–30, 2017.
- [26] F. Mogavero, A. Murano, G. Perelli, and M.Y. Vardi. Reasoning about strategies: On the model-checking problem. *ACM Transactions on Computational Logic*, 15(4):1–42, 2014.
- [27] P. Y. Schobbens. Alternating-time logic with imperfect recall. *Electronic Notes in Theoretical Computer Science*, 85(2):82–93, 2004.